Wind Tunnel Testing of a Low Reynolds Number Aerofoil

R. M. Lean

Fourth-year project in group C, 1995/1996

Cambridge University Engineering Department, 22nd May 1996

Contents

Summary

A full-scale wing section from a human powered aircraft was built and tested, in order to measure the position and qualities of the suction surface transition bubble. The profile drag of the aerofoil was evaluated using a wake traverse which was to be used in flight tests. The large size of the wing section meant that the wind tunnel walls had a significant effect upon the performance of the aerofoil at high angles of attack, although inviscid modelling of the flow prior to wind tunnel testing served to minimise this. Performance of the aerofoil in terms of profile drag and transition location was found to be close to the design requirements around the design point.

1 Introduction

1.1 Low Reynolds Number Aerofoils

Low Reynolds number aerofoils are a class of aerofoil sections which exhibit a number of unique qualities, and which occur in many important applications. However, they represent an area of aerodynamics about which little has been known until relatively recently.

Low Reynolds number aerofoils are generally defined to be those which operate at Reynolds numbers based on the chord length of 500,000 or below. Aerofoils designed specifically for use in this regime can give significant improvements in performance over more conventional aerofoils in certain applications. These include model aircraft[2], gliders, ultralight aircraft, wind turbines, propellers, high-altitude atmospheric sampling or reconnaissance aircraft and human powered aircraft (HPAs)[3]. The DAI 1335 aerofoil (fig. 1.1) tested in this study was designed for the MIT Light Eagle HPA (fig. 1.2), at a chord Reynolds number of 500,000[4]. This places it at the upper end of the 'low Reynolds number' regime, but nevertheless demonstrates many of the unique features of this family of aerofoils.

At low Reynolds numbers the flow is characterised by viscous effects, particularly by laminar separation of the boundary layer. Separation occurs because at low Reynolds numbers, transition does not naturally occur close to the leading edge. As a result, when the flow begins to experience the adverse pressure gradients associated with the pressure recovery region, the flow is still laminar. Due to its inferior ability to resist adverse pressure gradients, the laminar boundary layer then separates from the surface. This region of flow separation may continue to the trailing edge, or transition of the free

shear layer may result in reattachment of the flow and formation of a 'separation bubble'. The turbulent boundary layer is more able to resist further pressure gradients, and in many cases remains attached until the trailing edge.

The separation and transition process results in an increased momentum deficit in the wake, and thus increased friction drag. The form drag is also increased by the separation region, and the displacement effects can drastically alter the pressure distribution around the aerofoil compared with the inviscid case. The design philosophy for such aerofoils usually centres around minimising such adverse affects of separation.

1.2 Codes for Low Reynolds Number Aerofoil Analysis

Several design techniques have emerged through the years, which deal to a greater or lesser extent with the effects of extensive flow separation in this regime. One of the earliest began development at Delft University in 1966. This computer program[5] used conformal mapping to predict the potential flow and separate routines to predict the laminar and turbulent boundary layer regions. The e^n method was used to predict transition. This program, however, could not predict the all-important regions of flow separation, and pointed the way towards further research into this area.

A code known as MADAAM was extensively used by R H Liebeck at the Douglas Aircraft Company to design a series of aerofoils which have been used for numerous applications such as the Gossamer Albatross human powered aircraft[6]. This code was said to be well-calibrated in the low Reynolds number range, but was also unable to predict the effects of separation bubbles on the flow[7]

A more sophisticated code, developed by Eppler and Somers, became available in 1980[8]. This was capable of calculating a viscous pressure distribution which modelled a separation bubble. It was therefore capable of predicting the lift and pitching moment to a reasonable degree of accuracy, but was not capable of estimating the increase in drag due to the bubble. It gave a 'bubble warning' whenever a separation bubble was present, to indicate that the drag prediction was probably an under-estimate of the true value. The code which was used to design the aerofoil used in this experiment was presented by Drela and Giles in 1987[9]. This code, called ISES, was the first to predict the drag increase due to a separation bubble. It uses an e^9 type method to predict transition due to the growth of Tollmien-Schlichting waves as modelled by solutions to the Orr-Somerfield equation. A displacement method is used to couple the viscous and inviscid solutions. A slightly modified version of the ISES code, known as XFOIL, has been available since 1989[10].

Results from the ISES code have been verified in several experiments, and it has been

proven to be consistently more accurate than the Eppler and Somers code [11 12]. However, these results have indicated that in some areas, the prediction of the separation bubble is less than ideal.

1.3 Simulation of an HPA Wing in Wind Tunnel Tests

Wind tunnel tests to date have been centred around measurements of small-scale wind tunnel models of around 6" chord. These models, often accurately numerically machined from aluminium, do not represent the actual surface finish and contours found when the aerofoils are used in a human-powered aircraft application.

The generation of human powered aircraft which has emerged since the mid-1980's, of which John McIntyre's Airglow is a representative example, uses a very lightweight structure for the wings. This consists of carbon fibre spars supporting Styrofoam ribs which give the required aerofoil section. Areas of the wing where surface contours are critical, such as the forward area of the top surface, are skinned with thin Styrofoam sheet. Other areas are covered with heat-shrink Mylar film. The wing skins are thus very flexible. The achieved aerofoil shape is altered by deformation of the skins due to aerodynamic and structural loading, and the skin tension of the heat shrink film. The surface finish of the wing may also be less than perfect due to manufacturing techniques or surface contamination. Wind tunnel tests carried out in the past have not taken these effects into account.

This project was begun with the aim of testing a section of wing which represented as closely as possible the actual surface conditions of the DAI 1335 aerofoil in operation on the Airglow HPA.

The Airglow HPA has been instrumented to enable various performance parameters to be logged in flight[13] (fig. 1.3). A new instrument which has been built to enable further data to be gathered is a hot wire wake traverse which is designed to be mounted on the trailing edge of the wing. Due to the high aspect ratio of the wing, the flow on many locations along the span is effectively two-dimensional. The drag measured using this wake traverse in flight will thus closely represent the 2-D performance of the aerofoil section. This is an advantage as this is often difficult to measure by thrust or total energy methods due to induced drag, profile drag of the fuselage and empennage and ground effect.

2 Drag Reduction in Low Reynolds Number Aerofoils

2.1 Drag Increase Due to a Separation Bubble

The profile drag of a low Reynolds number aerofoil can be strongly affected by the presence of a separation bubble. This drag has two components: friction drag and form drag. A separation bubble can have the effect of increasing both these components (fig. 2.1), as described by Drela in reference [4], and summarised here.
The friction drag of an aerofoil is determined by the momentum thickness of the wake at the trailing edge of the aerofoil, as described by the equation:

$$C_{dv} = 2\left(\frac{\theta_\infty}{c}\right)$$

Thus, in order to minimise the friction drag, θ must be minimised. The value of θ is determined by the von Karman integral momentum equation:

$$\frac{1}{\rho u_e^2 \theta}\frac{d(\rho u_e^2 \theta)}{d\xi} = \frac{C_f}{2\theta} - \frac{H}{u_e}\frac{du_e}{d\xi}$$

It can be seen that the shape factor H influences the growth in momentum thickness. As a result, an area of flow separation causes an increased rate of θ growth, due to the increased shape factor in this region (fig. 2.2).
Skin friction is negligible in separation bubbles due to the very low velocity gradients in the stagnation flow. As a result, the skin friction term in the above equation can be eliminated, and the equation rearranged to give:

$$\frac{\Delta(\rho u_e^2 \theta)}{\rho u_e^2 \theta} = -H\frac{\Delta u_e}{u_e}$$

It can thus be clearly seen that in order to minimise drag, the separation bubble's length must be minimised (fig. 2.2).

2.2 Control of Separation Bubble Size

Separation bubbles could be avoided altogether by ensuring that the flow undergoes transition to turbulent flow before the pressure recovery is reached. However, this will not occur naturally without some form of stimulation at low chord Reynolds numbers. A trip in the form of surface roughness or a zig zag tape is often employed to accomplish this.

In this application, it was decided not to employ any form of 'trip' for two reasons. Firstly, human powered aircraft are often flown in the very early morning to benefit from the still air. At this time of day, however, dew or frost can often quickly accumulate on the wing's upper surface. This can result in a significant deterioration in a laminar flow aerofoil's performance, a phenomenon often observed on modem gliders. To remove the contamination, the wings are quickly wiped down before flight. Any form of trip stuck to the surface of the wing would not survive such treatment.
The second reason for avoiding a fixed transition device is that the separation point on the aerofoil moves according to the angle of attack. Thus, a fixed transition point would at some operating conditions be too far downstream to prevent separation, but at other times would be further upstream than was required. The skin friction and momentum thickness would therefore be higher than their optimum values at any point away from the design point.

The advantage of using the separation bubble as the means of causing transition is that the transition point can therefore move with the separation point, maximising the amount of laminar flow.

Transition often occurs in separated flow due to the increased growth rates of Tollmien-Schlichting waves in such regions (fig. 2.3). In order to minimise the adverse affects of the separation bubble, its size must be minimised by ensuring that transition occurs as quickly as possible following separation. In designing the DAI 1335 aerofoil, Drela used a strategy earlier employed by Wortmann[14] and Eppler.

The aim is to bring the boundary layer almost to the point of transition and hold it there, so that the flow is ready to go turbulent as soon as the flow separates. This is accomplished by making the laminar boundary layer undergo a gentle adverse pressure gradient in the region downstream of the leading edge. In this way, the velocity profile becomes inflected and instability growth is encouraged along this 'transition ramp'. The further increased shape factor of the separated region therefore quickly gives the small extra incentive which is needed for transition.

If the above strategy is employed in its purest form, the aerofoil is very susceptible to surface contamination or imperfections in the aerofoil contours over the transition ramp. as transition can be prematurely provoked As a result, the DAI 1335 employs a convex, gradually increasing adverse pressure gradient into the pressure recovery. In this way, transition is less likely to rush forwards in the event of deviation from the design operating conditions.

The DAI 1335 was one of the earliest aerofoils designed using the ISES code, and as such is relatively conservative. It is designed to operate with a separation bubble on its suction surface, this separation bubble being larger than optimum for minimum drag at the design point, but giving some insurance against premature transition due to surface

imperfections or errors in the design process.

3 Initial Design of the Experiments

3.1 Reasons for Wind Tunnel Testing

The key features of the aerofoil's performance to be examined in this investigation were the position and structure of the separation bubble, and the drag of the aerofoil over a wide range of operating conditions. It would thus be possible to test whether the aerofoil achieved its design objectives. The aerofoil has been proven in practice, in that it has been successfully employed both on the MIT Light Eagle and Airglow HPAs.

However, it has never been examined in detail in a wind tunnel.
Wind tunnel testing offers possibilities which flight testing cannot provide. For instance. in a wind tunnel the flow structure of the separation bubble can probed and measured more easily than it can be in flight. The operating conditions in a wind tunnel can be varied at will. The free stream turbulence intensity can be altered by disturbing the flow upstream of the test section, and the wing can be tested at angles of attack which cannot be sustained in flight.

3.2 Wing Section

Drela stated in reference 4 that the DAI 1335 was not tested in a wind tunnel because of the impossibility of replicating Light Eagle wing's surface finish on a scale model. A sufficiently large, low turbulence wind tunnel was not available to allow testing of a full-size section. For this study, it was decided that the wind tunnel facilities available at Cambridge University Engineering Department would permit testing of the section at full scale.

Full scale testing was attractive as the original surface finish could be exactly duplicated. The separation bubble would be much larger than that present on previous low Reynolds number aerofoil tests. This would allow a detailed examination of the separation and transition region. The full-size section would also allow testing of the new wake traverse, as mentioned in the Introduction and described below, in conditions closely representative of flight conditions.
The decision to test a full-scale wing section was based upon using the low turbulence wind tunnel with a 3'x 3' (approx. 0.9 x 0.9m) test section, and the Markham Low Speed Tunnel with its 5'6"x 4" (1.65 x 1.2m) test section. This important choice was made at the time of the decision to go ahead with the project, to allow time for the construction

of the wing section.

One wing section was built to be used for both sets of tests. The section was of constant (1.05 m) chord with the DAI 1335 aerofoil, representative of the centre section panel of the Airglow HPA. The span was 5'6" (1.69 m) to fit the span of the Markham wind tunnel. In order to reduce the cost and make the wing more robust, the internal structure was built from wood rather than the original carbon fibre spar and Styrofoam rib construction. The wing skins, however, were faithful reproductions of the original, built using the same materials and techniques. The result was a test piece which accurately represented the wing contour and surface finish of the Airglow wing. The only concession was that the trailing edge, built from wood, had a finite thickness of around 2 mm as compared with the sharp composite trailing edge of the original.

3.3 Measurement of Aerofoil Performance

Measurement of the flow was to be carried out using constant temperature hot wires. In the first set of tests, the hot wire would be mounted on a computer controlled, movable probe to examine the separation and transition regions. In the second tests, the wake traverse would cycle the wire at constant speed up and down through the wake. As is often the case, the chosen test techniques present some difficulties. Previous low Reynolds number aerofoil tests have shown that vortices often form at the junction between the wing section at the tunnel wall, spoiling the two-dimensionality of the flows. Some facilities allow the application of mild suction to correct this, but due to the relatively short time and low budget available for this experiment, this was not possible. As a result, there would only be a relatively small area of two-dimensional flow towards the centre of the test section. Any measurements would thus need to be taken in this region. Measurements from a force balance attached to the wing would have little meaning due to the variation of the flow across the span. This is not a serious problem as the main areas of interest for this study are the measurement of drag and examination of the flow structure.

The proximity of the wake traverse to the wing was also a cause for some concern. It was feared that the bulk of the traverse gear mounted on the trailing edge of the wing would affect the pressure field on the nearby wing surface, thereby affecting the drag measurements. Secondly, the calculation of the profile drag coefficient relies on a measure of the momentum deficit in the wake at infinity downstream (equation 1). The point of measurement using this wake traverse is only approximately 5% of the chord length downstream of the trailing edge. At this point, the static pressure has not yet fully recovered to atmospheric value. This makes calculation of the wake at infinity difficult,

as the traverse is not equipped to measure the static pressure as well as the flow velocity. A previously discovered problem with the wake traverse method of drag measurement on low Reynolds number aerofoils is due to the unsteady nature of the wake of an aerofoil with flow separation. However, this problem is the most evident with a wake rake pitot and manometer method, where the measured value of dynamic pressure fluctuates with time. The wake traverse employed in this experiment allowed many different wake profiles to be quickly measured. In this way, the mean profile could be calculated for use in drag estimation.

4 Description of the Experiments

4.1 Low Turbulence Wind Tunnel

The low speed transition research facility was used at Cambridge University Engineering Department shortly before its removal to Queen Mary and Westfield College, London. This closed return tunnel has a 25 hp do motor driving an axial fan. The flow is smoothed through honeycombs and changeable screens before undergoing a 9:1 contraction into the 3' x 3' (0.92 x 0.92m) interchangeable working section. The tunnel was designed to give a very low turbulence intensity, and is often used for transition experiments on flat plates.

One of the interchangeable working sections was modified to accept the large wing. The wing was mounted with its spanwise axis vertical to allow the hot wire probe which is usually used for flat plate transition experiments to probe the suction surface. Being of 5'6" span, it was necessary to cut through the roof of the tunnel to allow 2'6" of wing to protrude above the working section. The wing was bolted to the tunnel floor at its bottom end and a steel frame at its top end. A seal was made around the junction of the wing and the tunnel roof which allowed the wing to be rotated to different angles of attack in between runs.

The large size of the wing relative to the test section meant that the tunnel walls affected the pressure field around the wing. If great enough this blockage effect could significantly alter the performance of the test aerofoil, rendering the results of the tests useless. A panel code was written to predict the effects of the proximity of the tunnel walls on the inviscid flow around the aerofoil. A brief description of this code can be found in Appendix A. It was important to check that the pressure gradients over the top surface of the wing were not too strongly affected by the wind tunnel walls as these could alter the position and structure of the separation bubble.

On first running the code, it was discovered that mounting the wing on the centreline of the tunnel would give unacceptable deviations from the intended pressure

distribution. As the angle of attack was increased, the leading edge approached the tunnel side wall, causing a premature pressure spike to form. Streamlines which would be curved with the wing in free flight were constrained to be straight by the sides of the tunnel. As a result, some form of modification was required.

It had been suggested that contoured foam pieces could be cut to modify the shape of the tunnel walls to fit the curved streamlines. The required streamline shapes close to the walls could be calculated using the panel code, then foam pieces cut to this shape and stuck to the tunnel walls. This would give the required pressure distribution around the wing. However, different pieces would be required for each angle of attack to be tested. The foam pieces could obstruct the traversing hot-wire probe which protrudes through one wall. Boundary layer problems such as flow separation could arise on the curved pieces if the required curvature were too great. Furthermore, time was a restricting factor, as only a few weeks were available to prepare for the tests before the wing tunnel was removed.

Therefore it was decided that a simpler solution was required. The panel code was run with the wing in different positions in the test section. It was found that by moving the wing 0.25m from the tunnel centreline, a greatly improved flow resulted over the suction surface of the wing. There was more space between the suction surface and the tunnel wall, meaning that the flow near to the wing was far less constrained. The premature pressure spike was eliminated within the working range of angles of attack. The flow on the pressure surface of the wing was altered, resulting in increased circulation around the wing as a whole, but this was not too critical as it was only the suction surface flow which was of interest in this experiment. The predicted pressure distribution using this modification was still not perfect as the adverse pressure gradient on the transition ramp was greater than that required. However, given the time and resources available, it was the best solution which could be found.

A further modification to the tunnel was made due to the displacement of the wing away from the centreline as viewed from the probe traverse gear. As mentioned before, the probe is usually used for measurement of boundary layer flows on flat plates which are mounted on the tunnel centreline. As a result, the existing probe was too short to reach the aerofoil's surface, especially towards the trailing edge with the wing at a high angle of attack. As a result, a new probe was built which was long enough to reach almost to the far wall of the working section, in anticipation of future experiments. The Dantec hot wire mounted on the end of the probe was used with an overheat ratio of 1.6. The hot wire was connected to a 55M01 constant temperature anemometer unit, and the output signal split into AC and DC components and the AC component amplified by a factor of between 500 and 12.5 depending on laminar or turbulent flow. The amplified signal was logged by computer via an INT 16 analogue to digital

converter, or displayed on an oscilloscope.

The wind tunnel is equipped with an Acorn Archimedes computer. This is used to control the tunnel speed and hot wire position. It is also capable of receiving and logging data from the hot wire anemometer. As a result, it is possible to write codes to fully automate many of the required functions of the tunnel such as hot wire calibration and wake profile measurement. A number of standard routines have been accumulated over the years, although many of them are only applicable to flat plates with Blasius profiles. As a result, a few new routines were written tailored to the requirements of this experiment.

A new problem presented itself due to the unusual nature of the wing being tested. Measurement of the separation bubble involved the production of boundary layer profiles at different points along the chord of the wing. This requires the wing's surface to be accurately located so that the hot wire probe does not ground itself, breaking the wire and damaging the delicate surface finish of the wing.

On transition experiments involving a metal flat plate, finding the surface is a simple matter. Being flat, the surface is a constant distance from the tunnel wall. The edge of the boundary layer can be accurately located assuming a Blasius velocity profile, and confirmation of reaching the surface is contained when the proximity of the metal plate causes a spike in the hot wire signal. None of these advantages are available when using a curved, non-conducting surface.

An initial idea was to write a program which used the aerofoil co-ordinates to locate the surface for a given angle of attack. However, this would not locate the surface to the required level of accuracy. Similar results could be by obtained using a much simpler program which stepped the wire in towards the wing with the tunnel running. The boundary layer could be located when the mean velocity fell to a certain proportion of its free stream value.

It was found that contact with the surface, which was coated in Mylar, had no discernible effect on the hot wire signal. A measured mean velocity of zero could not be used as a criterion either, due to the very low magnitude velocities found away from the surface in a separation bubble. As a result, it was decided that before beginning each test, it was necessary to stop the tunnel, climb inside the test section and locate the hot wire on the wing's surface by eye. It was possible to do this very accurately by stepping the probe towards the wing until the reflected image of the hot wire and the wire itself became one. In this way, the surface of the wing could be located to within 0.1 mm. Stopping the tunnel after producing each boundary layer profile was less than ideal. It was time consuming having to open the tunnel, climb in and manually locate the probe on the surface. It required two people to be present, one to watch the probe and one to move it using the computer. Furthermore, the tunnel had to be run up to speed each

time, and some care was necessary to ensure that the same chord Reynolds number was achieved for each run. However, no easier method has been found. A conductive coating on the wing would allow the surface to be found automatically using a computer routine. The reason why this was not used is that the conductor would alter the surface finish of the wing, rendering useless all of the efforts to achieve a representative surface finish.

A routine was written to step the hot wire probe away from the wing 0.2 mm at a time, measuring the mean velocity and turbulence intensity at each location. In this way, boundary layer profiles were built up for different positions along the chord.
Calibration of the hot wire was accomplished by traversing the probe to a location downstream of the wing to a position calculated by the panel code where the flow velocity was calculated to be equal to the free stream value. The hot wire was calibrated against measurements from a pitot-static tube which was read by the Archimedes via a pressure transducer and fNT 16 interface.
As well as mean velocity and turbulence profiles, spectra of the turbulence intensity within the boundary layer were produced by data logging at 4 and 20 kHz using a 486 laptop PC.

Experiments were run at the design Reynolds number of 500,000 at angles of attack of 0 and 4 degrees. 4 degrees represented the design operating point of the aerofoil on the Airglow HPA. 0 degrees was chosen as it would demonstrate movement of the separation bubble, while minimising the unwanted interference effects of the tunnel walls.

4.2 Markham Low-Speed Tunnel

The Markham low-speed wind tunnel wind tunnel has a 5’6” x 4’ (1.69 x 1.23m) working section. Its 100 hp electric motor is capable of producing velocities of up to 200 ft/sec (61.5 m/s). The tunnel is used for many different applications, and is not designed to provide the extremely low free stream turbulence intensity from which the Low Turbulence tunnel benefits. However, it has a larger working section than the previously mentioned tunnel and thus suffers less from blockage effects than the other tunnel.

The wing was mounted inverted with its spanwise axis horizontal. It spanned the entire test section, and the gaps between the tips and the perspex side walls were padded with low density plastic foam which was cut to the aerofoil section and stuck to the wing. This was done to eliminate tip vortices due to flow spillage between the top and bottom surfaces, making the flow as two-dimensional as possible.

The wing was suspended on the wires of the tunnel's force balance. The balance can measure lift, drag and pitching moment. In this case, the drag forces were predicted to be far too low to be accurately measured using the balance which is intended for models operating at much higher speed.

The lift and pitching moment were measured, but the results are not presented in the main body of the report. This is for two reasons. The first because the flow was not uniform and 2-D across the whole span, due to vortices at the end walls and turbulent wedges downstream of mounting wires for the balance. The second is due to the friction between the foam padding and the tunnel side walls with the test section doors closed. The friction created meant that most of the movement of the wing was taken up in shear of the approximately 1 cm thick foam. The balance was calibrated in this condition, but the results are not thought to be of sufficient accuracy due to possible slippage of the foam against the wall causing a hysteresis effect.

The wing was suspended at two points on its 25% chord line, and at one point towards the trailing edge. The model being mounted inverted, the lift acts downwards as long as the lift coefficient is positive. Generally in this tunnel, weighted 'down-wires' hang below the test model to prevent it flying away in the event of a negative lift coefficient being encountered.

In this experiment, any down wires would have to pass through the suction surface of the wing, ruining its surface finish and providing an opportunity for flow leakage between the top and bottom surfaces. It was predicted that the range of lift coefficients which would occur was positive, with a minimum of 0.5. Friction from the foam pads at the wing tips was an extra safety measure which would prevent the wing moving in the event of anything unexpected, and the low tunnel running speed meant that dynamic forces were generally low. For these reasons it was decided not to use down wires for this experiment.

The wires on the pressure surface of the wing were expected to create turbulent wedges downstream. The positions of these wedges was calculated in order to place the wake traverse in an area free from such disturbance. A worst case scenario was calculated with a wedge angle of l8 degrees. This was an extremely pessimistic estimate which also took into account the disturbance on the wing skin around the area where the wire mountings passed through the wing's surface. It was very unlikely that the wedges would be this large as a favourable pressure gradient exists over most of the pressure surface at positive angles of attack. The prediction left very little space on the trailing edge which was free of the turbulent wedges. The traverse was placed mid-way between two predicted turbulent areas, 0.l m offset from the wing centreline.

The wake traverse was designed to be mounted on the trailing edge of the Airglow aircraft. A constant temperature hot wire is cycled continuously at constant speed

perpendicular to the flow direction on a high precision lead screw driven by an electric motor. The hot wire is held on a carbon fibre tube in the clear air to one side of the aluminium traverse gear structure and its mountings.

The unit is powered by NiCad batteries in flight, but a dc power supply was substituted for the wind tunnel tests. The unit outputs two signals: a square wave indicating the motor direction and the hot wire voltage. The hot wire was driven by a single board anemometer unit, and both signals were logged on a 486 laptop PC using an ADC 11 analogue to digital converter and Picolog software. This gave a resolution corresponding to approximately 0.01 m/s. A 50 Hz sampling rate was used as it was the mean velocity component that was important for drag measurements.

The hot wire was calibrated with the wing at 0 degrees incidence and the traverse gear driven to its furthest extent away from the wing on the pressure surface side. This was to ensure that it was as far into the free stream flow as possible. A small correction factor was applied due to the static pressure error at this point relative to that at infinity.

Measurements were made over a range of different angles of attack for a number of different conditions. The free stream turbulence intensity and surface finish were varied to simulate different meteorological conditions and wing surface contamination. These would affect the transition location and thus the measured drag. All tests were done at a free stream flow velocity corresponding to a chord Reynolds number of 500,000. Each data point represents one tunnel run. Due to the friction of the foam wing tips against the tunnel walls, the tunnel was stopped, the doors opened and the wing's alignment checked with a digital inclinometer for each new angle of attack. The tunnel was then run up to the required speed as indicated by the tunnel's digital manometer. The speed was stabilised at the correct value before readings were taken to ensure that the chord Reynolds number was consistent. The wake traverse was run and the computer logged the results for two runs each of 90 seconds. This corresponded to 20 wake profiles. The lift and pitching moment values were noted while the traverse was running.

The first set of data was collected with a clean wing and the wind tunnel's natural free stream turbulence intensity. Angles of attack from 0 to 10 degrees were measured in 1 degree steps.

The second test type involved increasing the turbulence intensity in the tunnel by means of a turbulence screen. This consisted of a wooden lattice of 20 mm square bars at 100 mm pitch. This existing piece of equipment represented a very high free stream turbulence intensity, ensuring turbulent flow on the entire wing's surface. Five points between 0 and 10 degrees were measured.

The third set of runs used a more realistic turbulence screen. This was achieved using string of 1.5 mm diameter in a square grid of 150 mm pitch upstream of the test section.

Seven measurements between 0 and 10 degrees were made.
The fourth experiment involved a clean wing with the tunnel's standard free stream turbulence intensity. One of the foam pieces was removed from one wing tip to allow the cycling of the wing angle of attack with the tunnel running. The reason for this was to allow investigation of a hysteresis effect in the lift curve which has previously been observed in low Reynolds number aerofoils [16]. However, it was extremely difficult to change the angle attack of the wing while keeping the tunnel free stream velocity constant. as changing the angle of attack had a significant effect on tunnel blockage.

Drag measurements were made during these tests to investigate the effect of small gaps at the tunnel walls on the 2-D profile drag measured at the centre section.
Attempts to alter the surface finish of the wing at first proved to be unsuccessful. The most common form of surface contamination is dew which forms in the early mornings on the top surface of the wing. It had been hoped to simulate this directly using a water mist sprayed onto the wing before each run. However, the relatively warm conditions within the tunnel (22 degrees Centigrade) meant that the water droplets quickly evaporated when the tunnel was run. Therefore, an alternative had to be found.
The solution eventually tried involved using matt Letra cote from an aerosol to simulate the very fine water droplets. This was sprayed as evenly as possible onto the wing suction surface. The final tests involved running the wing at close to its operating angle of attack and measuring the effect on the drag values.

5. Experimental Results and Analysis

In this section, the experimental results are presented and compared with predictions of performance from XFOIL, a slightly more modem version of the Drela and Giles ISES code which was originally used to design the DAI 1335 aerofoil. In this program, the user is able to define the value of n, the critical amplification factor of the Tollmien-Schlichting waves in the boundary layer. The program gives an indication of the rms free-stream turbulence intensity which this value represents. In this way, it was possible to simulate the turbulence conditions in each wind tunnel test by varying the value of n.

5.1 Low Turbulence Wind Tunnel

The measurements from the Low Turbulence Wind Tunnel allowed plots of mean velocity and turbulence intensity profiles to be created for the central region of the suction surface of the wing. The plots clearly show the progression from a classic laminar profile, through an inflected profile to one of separation, then reattachment as a fully turbulent boundary layer (fig. 5.1.1, 5.1.2).

The shape of the bubble as deduced from the zero velocity line on the mean velocity profiles (fig. 5.1.3) follows the classic form of a short separation bubble as has been measured previously, with its gradual gradient at its leading edge, and the more abrupt reattachment following transition to turbulent flow.
Separation bubbles were detected at both angles of attack measured. However, the proximity of the tunnel walls still had some effect upon the boundary layer behaviour as indicated by the panel code.

At 0 degrees, the location of the bubble is close to that predicted by the Drela code. Free transition, as marked by a peak value of the shape factor H, was observed to occur at x/c = 0.553 (fig. 5.1.5) compared with a predicted value of 0.582. However, the extent of the separation is reduced from its theoretical value, as indicated by a reduced peak in the shape factor H. XFOIL predicts a peak value of H = 7.3 when run with the critical disturbance amplitude n = 9. However, measurements indicated a peak shape factor of only H = 4.7.

At an angle of attack of 4 degrees, the difference between theory and experimental data is similar, with separation and transition again happening slightly upstream of the predicted location. The XFOIL code predicted free transition at x/c = 0.537, whereas measurements indicated this to occur at x/c = 0.507 (fig. 5.1.6). The peak value of H was reduced, at 4.2 as compared with a predicted value of 5.7.

It must be noted that the values for the shape factor H in the separation region output by XFOIL cannot be directly compared with those calculated form hot wire boundary layer data. The reason for this is that the hot wire anemometer measures the modulus of the velocity and not its direction. Thus, XFOIL calculates the boundary layer parameters on the basis of reverse flow in the separation region, whereas the hot wire measured a low positive velocity in this region. The result is that XFOIL will always output a higher value of H in a given region of flow separation than hot wire measurements will indicate. Because of this, it is difficult to tell how much the degree of separation differs between the two sets of results.

These results indicate that the proximity of the tunnel walls did indeed affect the performance of the boundary layer. In both cases, the steepened adverse pressure gradient on the transition ramp had the effect of provoking separation of the laminar boundary layer 3% of the chord upstream of the predicted position. It also possibly increased disturbance amplification on the transition ramp. resulting in a smaller bubble once the flow did separate.

It can therefore be concluded that the model was a little too large for the tunnel, and that the correction applied by moving the wing away from the tunnel axis did not go far enough to correct the pattern of the flow.

Vibration of the model was observed. The wing skin on the pressure surface close to

the tunnel floor and roof was seen to oscillate when the tunnel was running. This type of vibration has not been observed in flight on the Airglow aircraft. It therefore probably indicates some sort of interaction of the wing with the tunnel boundary layers, and possibly the type of low Reynolds number vortex that has been observed previously. The vibrations, if of the correct frequency, would have the effect of increasing the amplitude of the disturbance growth in the boundary layer and thus provoking earlier transition. This would reduce the streamwise length of the separation bubble.
The progression from laminar to turbulent flow can be observed using the mean velocity profiles and the turbulence intensity profiles through the bubble (fig. 5.1.3. 5.1.4). The turbulence intensity grows the most rapidly in the boundary layer above the stagnation region, and the increased amplification rate in the separated region can be clearly seen in the plot of rms turbulence intensity.

Frequency spectra taken in the boundary layer at an angle of attack of 4 degrees show clear peaks at around 200 Hz in the laminar boundary layer. These peaks are not at all evident at x/c = 0.279, but are clearly present in the region just upstream of separation. at x/c = 0.483 (fig. 5.1.7). This shows that these waves were not present in the tunnel's free stream turbulence, and have been amplified in the boundary layer. The frequency of the waves is seen to slightly increase with distance downstream, confirming that the critical frequency for amplification is a function of Reynolds number.
The transition from laminar to turbulent flow is a gradual process, as can be seen from the steadily increasing level of noise in the turbulence spectra. The amplitude of the noise grows to swamp the 200 Hz and 400 Hz peaks as the flow moves downstream through the separation region. These peaks can, however, still be found at x/c = 0.597 where the flow is fully developed into a turbulent boundary layer profile.
A series of turbulence spectra through a cross-section of the upstream end of the bubble at x/c = 0.447 reveals that the region of the boundary layer closer to the surface retains a laminar-type frequency spectrum longer than that further away. where turbulent flow is already beginning to evolve (fig. 5.1.8).

5.2 Markham Low-Speed Tunnel

The most important set of measurements in this set of experiments is the data from the hot wire wake traverse which was fitted to the trailing edge of the wing. An example of a typical wake profile can be found in fig. 5.2.1. The raw data was processed using the program described in Appendix B. This output figures for the two-dimensional drag coefficient of the aerofoil. These results are plotted in fig. 5.2.2.

Comparison with the predicted values from XFOIL using the same measured free-

stream turbulence intensity values indicates good agreement between the theory and experimental results for low and moderate angles of attack. At higher angles of attack the measured drag was lower than that predicted by the computer program.
The free stream turbulence intensity in this wind tunnel was measured to be 0.26%. This corresponded to a critical value of n = 5.85. The measured values of drag were up to 10% lower than the predicted values for angles of attack up to 5 degrees. At 6 degrees and above, the drag rise predicted by XFOIL was not observed to the same extent in the experiments. This effect increased until at 10 degrees, the measured values were only 50% of those predicted.

The turbulence intensity was increased by the string mesh to a value of 1.25%, corresponding to n = 2.09. The results of this test show less agreement than those at the lower turbulence intensity value (5.2.3). The measured drag was up to 30% higher than that predicted by the computer model for angles of attack of 6 degrees and below. Above this, the experimental data again exhibits a sustained low drag level where XFOIL predicts a drag rise.

A possible reason for this is that the frequency spectrum of the turbulence created by the grid was significantly different from that assumed by XFOIL. A second possibility is that the turbulence intensity experienced by the wing was not completely uniform due to the wide spacing of the string in the turbulence grid. This could give rise to three-dimensional effects. It is possible that the increased turbulence intensity resulted in transition without separation, and that the increased drag at low angles of attack is caused by there being more turbulent flow on the wing than predicted.
However, the change of the pressure surface boundary layer from laminar to turbulent flow at the trailing edge occurred in both the computer and wind tunnel experiments between angles of attack of 4 and 5 degrees. This could be observed in the experiment by examining the boundary layer profiles as seen in the wake traverse results.
Only three runs were possible with increased surface roughness, due to time constraints. The results, taken with an unobstructed free stream, show that the low level of contamination introduced to the wing's suction surface had no measurable effect on its drag performance.

Two reasons have been put forward for the measured drag figures being lower than the predicted ones for angles of attack above around 5 degrees. The first reason is again interaction between the tunnel floor and ceiling and the wing. Although the Markham tunnel's test section is larger than that of the Low-Speed wind tunnel, the wing was this time mounted close to the centreline of the test section. As a result, the distance from the tunnel floor to the wing's suction surface was similar to that in the Low Turbulence tunnel. The overall circulation of the wing was not as badly affected with this set of tests as it was previously, but nevertheless, the slope of the lift curve has been significantly

altered. The wind tunnel has therefore again had the effect of increasing the strength of the adverse pressure gradients. reducing the size of the separation bubble on the suction surface of the wing. Separation bubbles were observed on the suction surface in all of the computer simulations, indicating that there was still scope for drag reduction due to diminishing the bubble size.

A second possible explanation for the reduced measured drag is due to the positioning of the hot wire on the wake traverse. As the angle of attack was increased, the thickness of the boundary layer at the trailing edge of the suction surface increased to the extent that the range of hot wire movement did not include the entire boundary layer. This effect was, however, small, and it is estimated that at the higher angles of attack the contribution of this effect would be no more than 5% in the worst case.

A test was run with the foam seal removed from one wing tip. This had the effect of introducing a gap of approximately 8 mm at one wing tip. The effect of this gap upon the drag measured by the wake traverse close to the centreline was small (fig. 5.2.2). It appeared, however, to slightly reduce the profile drag as compared with the case with the tips sealed. This is possibly due to slightly increased spanwise flow which could again provoke increased amplification in the laminar areas, and thus a reduced separation bubble.

Removal of one tip seal permitted the angle of attack to be adjusted with the tunnel running, with the aim of detecting any hysteresis in the lift curve. This, however, was not observed due to the difficulty of keeping the tunnel speed constant while adjusting the angle of attack. The means of changing the angle of attack did not allow a very smooth movement to be made, and the wing oscillated more and more as the angle was increased. It is very likely that these factors combined to eliminate any possibility of hysteresis. Previous experiments have shown that the flow is very sensitive to disturbances, and that even a knock on the tunnel wall was enough to remove the hysteresis effect[17].

The oscillation of the wing at higher angles of attack indicated the presence of an unsteady wake. This effect has been observed previously in low Reynolds Number aerofoils[8]. It is possible that the cause of this was a combination of tip vortices due to the gap at the end wall as well as unsteady flow in the aerofoil boundary layer. Evidence that the unsteadiness was a result of the two-dimensional aerofoil was provided by the varying shape of the wake profiles which were measured by different passes of the wake traverse. This was especially noticeable at angles of attack above 8 degrees. possibly indicating the onset of trailing edge separation.

An interesting addition to the measurements taken by the computer was the use of a pitot tube attached to a stethoscope to examine the boundary layer. The wake traverse was confirmed to lie in a region of clear flow. It was well outside the region affected by

the turbulent wedges downstream of the wire attachment points. These wedges were much narrower than the 18 degrees which had been used as the worst case for calculations. The flow even seemed to re-laminarise downstream of the forward wires, due to the favourable pressure gradient on the pressure surface.

Using the stethoscope. not onh could the difference between laminar and boundary layers be clearly distinguished, but also clear tones could be heard in the region around transition on the suction surface. These tones are thought to coincide with the peaks observed in the frequency spectra measured in the Low turbulence wind tunnel tests. By varying the wind tunnel speed, it was possible to change the chord Reynolds number. At a Reynolds number of 300,000. transition was observed to have moved back and the frequency of the tones was noticeably reduced compared with the case at Re = 500,000.

This type of observation was found to be extremely valuable in helping to gain a better 'feel' for the processes involved in boundary layer transition.

6. Concluding Remarks

The experiments carved out for this study have highlighted the difficulties of testing a large wing model at low Reynolds numbers. The interference effects of the tunnel upon the pressure distribution were seen to have significant effects on the behaviour of the boundary layer at higher angles of attack. This effect was manifested in increased lift and reduced drag as compared to the predictions of the XFOIL code, which can be expected to be highly accurate.

In retrospect, a half scale model would have been able to provide a reasonable degree of accuracy in reproduction of the surface finish, with a much lower cost in terms of the effects of the wind tunnel upon the measured performance.

The position of the wing in the wind tunnel can make a significant difference to the wing-tunnel interference effects, and it has been shown that simple inviscid modelling can be extremely useful in designing a rig prior to testing.

In the range of angles of attack where the tunnel interference effects were less significant, reasonable agreement was achieved theory and practice. The transition location on the wing was observed to be 3% of the chord ahead of its predicted location at angles of attack of 0 and 4 degrees.

Drag measured by the wake traverse and that predicted by XFOIL showed good agreement at angles of attack below 6 degrees for the case with free stream turbulence of 0.26%. The measured drag was higher than that predicted by the computer code for the case with free stream turbulence of 1.25%, possibly due to the frequency distribution

of the turbulence.

The importance of correctly positioning the wake traverse has been demonstrated, as has the need for some way of measuring the static pressure at the hot wire position. This would allow more accuracy in the drag calculations, although the weight and cost of a suitable pressure transducer may be prohibitive for application on the Airglow HPA. An alternative is to use the static pressure predictions from the XFOIL program, as was done in this case.

The importance of the free stream turbulence upon the performance of the aerofoil has been demonstrated. Slight increases in the turbulence intensity can result in drag reduction due to reductions in the size of the separation bubble. Significantly increased steady-state free-stream turbulence results in increased aerofoil drag, possibly due to transition ahead of the position for laminar separation. The importance of the frequency spectrum of this turbulence was also noted by the disagreement between the XFOIL and measured results for a turbulence intensity of 1.25%.

At the time of writing, flight testing of the wake traverse on the Airglow HPA is about to begin. The computer code developed during this project will be used for the analysis of the flight test data. This new data will make an interesting comparison with that measured in the wind tunnel.

Acknowledgement

This project would not have taken place without the help of the Airglow HPA team: John McIntyre, Mark McIntyre and Nick Weston. The author would like to thank them for providing the wing model and wake traverse for the experiments. Special thanks are due to John McIntyre for all of the help which he has provided in his spare time throughout the year, and for the privilege of being able to speak at the Human Powered Aircraft for Sport Conference at the Royal Aeronautical Society in January 1996.

Nomenclature

C	= aerofoil chord
C_f	= profile lift coefficient
C_d	= profile drag coefficient
C_f	= skin friction coefficient
Cp	= pressure coefficient = $\frac{2(p-p_\infty)}{\rho u_\infty^2}$
H	= shape parameter = $\frac{\delta^*}{\theta}$
n	= exponent of most amplified Tollmien-Schlichting wave amplitude
R_e	= chord Reynolds number = $\frac{\rho U_\infty}{\mu}$
u	= flow velocity
u_e	= boundary layer edge velocity
U_{te}	= boundary layer edge velocity at trailing edge
U_∞	= free stream velocity
x,y	= chordwise normal co-ordinates
α	= aerofoil angle of attack
δ^*	= displacement thickness = $\int(1-\frac{u}{u_e})d\eta$
θ	= momentum thickness = $\int\frac{u}{u_e}(1-\frac{u}{u_e})d\eta$
ρ	= air density
μ	= air viscosity
ξ,η	= boundary layer co-ordinates

Appendix A: Inviscid Flow Modelling of Wing in Wind Tunnels

An inviscid panel code was written in FORTRAN to predict to a first approximation the characteristics of the floes in the wind tunnel test section with the large wing panel in place.

This code was written using the commonly applied technique of modelling objects using a distribution of discrete vortices placed around the solid surfaces". The strengths of the vortices were solved to give the condition of zero flow perpendicular to the surface at target points which were placed mid-way between pairs of vortices.
In this way, the aerofoil section and tunnel walls were positioned in the flow. Co-ordinates for the working sections of the Low-Turbulence and Markham wind tunnels were used. The position and angle of attack of the wing could be varied at will. 81 vortices were used to model the wing, and 25 for each wind tunnel wall.

On each run, the program produced solutions for the flow around the wing in free flight and within the wind tunnel. Output was in the form of streamline visualisation and velocity and pressure plots around the aerofoil's surface. In this way, the characteristics of the two flows could be compared. The aim was to move the wing within the test section to make the aerofoil's performance inside the tunnel as similar as possible to that in free flight.

Many problems were experienced in applying the Kutta condition at the trailing edge of the aerofoil. Several different strategies were employed in an attempt to obtain a correct solution.

The problem each time was that the calculated strength of the vortices around the extreme trailing edge of the aerofoil was extremely high. This resulted in the flow being accelerated strongly around this area, resulting in an unwanted pressure spike. The effect can be seen in the streamline plots, where the streamlines converge around the very trailing edge.

The first technique attempted involved modelling the trailing edge as a very short panel, as if (as occurs on the wing used) the trailing edge is not a sharp point, but a squared-off shape. Solving the flow to give no normal flow or no tangential flow at the target point on the centre of the trailing edge had similar results.
A second attempt involved modelling the trailing edge as a sharp point. then placing a further panel behind the trailing edge, representing an infinitely thin panel which bisected the trailing edge angle. Solving for the zero normal flow condition in the normal way produced similar results to the first mentioned methods.

The final method which was attempted involved solving the flow, twice for total circulations around the wing of 0 and 1 respectively[20]. The system is linear, and therefore a weighted combination of the two solutions can be used to produce a solution

of any chosen net circulation. The required circulation was chosen using the requirement that the strength of the trailing edge vortices on the top and bottom surfaces must be equal and opposite. Again. the results were similar to those achieved previously.
The problem appeared to lie in the proximity of the vortices at the trailing edge. If the trailing edge was made very square and thick, the pressure spike disappeared. Removing vortices at the trailing edge went some way to improving the situation. Another possible solution which was not tried involved using far more vortices around the trailing edge region.

Each attempted solution produced similar results, which suggests that the problem did not lie in the area being investigated. However. due to time constraints a perfect solution was not found. The inaccuracies in the flow modelling occurred around the trailing edge, and the important region in terms of modelling the flow was near to the leading edge. The total circulation predicted by the program was correct, and as a result disproportionate amounts of time were not spent in trying to arrive at a prefect solution. Experimentation with the program resulted in the decision to move the wing 0.25m away from the centreline of the Low Turbulence tunnel, resulting in much improved performance of the wing in the ensuing series of tests.

Appendix B: Profile Drag Calculation

The profile drag of an aerofoil is related to the momentum deficit in the wake at infinity behind the trailing edge by the following equation:

$$C_{dv} = 2\left(\frac{\theta_\infty}{c}\right) \qquad (1)$$

Squire and Young related this to the momentum deficit at the trailing edge using the following empirical relationship:

$$C_{dv} = 2\left(\frac{\theta_{TE}}{c}\right)\left(\frac{U_{TE}}{U_\infty}\right)^{\frac{1}{2}(H_{TE}+5)} \qquad (2)$$

This formula was used to estimate the profile drag of the aerofoil using the wake profiles measured bN the hot wire anemometer mounted on the wake traverse gear 0.05m downstream of the trailing edge of the wing.

The raw data was of the form of two signals. One was a square wave indicating the current sweep direction of the probe, and the other was the voltage from the hot wire probe. King's Law was used to relate the flow velocity to the voltage E:

$$E^2 = A + BU^n \qquad (3)$$

where A and B are constants calculated by calibrating the hot wire before each set of tests, and n = 0.5. This is sometimes now regarded as a rather crude approximation, but for this application the accuracy was considered to be sufficient.

The traverse gear moved the wire at slightly different speeds in the up and down directions, although these speeds were in themselves consistent. It would have been possible to combine the results from the two motor directions to produce a single profile. However, it was decide to calculate results for both directions separately, as a comparison between the two results would give a useful means of verifying the results. Between 8 and 10 profiles had been recorded for each data point in each direction. The first job was to isolate the profiles from each direction, and then to produce an ensemble average by combining all the results from a given direction. Incomplete profiles at the start and finish of each run were discarded.

The next task was to find the edges of the wake and calculate the external velocity U_{TE}. A number of methods were attempted before a satisfactory solution was found. The problem lay in calculating a mean external velocity when there was appreciable free-stream turbulence and where the mean velocity gradient is very low on the edge of a turbulent velocity profile. In this way, it was difficult to identify what should be counted as being outside the wake.

A final solution was adopted which involved smoothing the velocity profile using a centred mean of 10 points for each point, then finding the point where the smoothed value fell below 0.99 of the mean value encountered outside this point.
The next problem was that the static pressure was not equalised at the measuring location close to the trailing edge. It had been anticipated that the pressure would not have recovered to its free stream value so that $U_{TE} \neq U_{\infty}$. However, what was unexpected was that the value of U_{TE} , was different either side of the wake. The external velocity on the suction side of the aerofoil was higher than that on the pressure side for all angles of attack measured. The static pressure at the probe location had not been measured, and as a result some form of allowance was required to calculate a value for U_{TE} to be used in the calculation of θ_{TE}

A value representing the mean of the two edge of boundary layer velocities was initially used. This was rather arbitrary, however, and the chosen location of the edge of the wake was critical as the difference between the mean external velocity and the actual

external velocity had an effect on the value of θ_{TE} , which was calculated.
The next approach was to linearly interpolate through the wake between the two values of U_{TE} . This was ineffective as the gradient of the interpolation closely followed the velocity gradient in the turbulent suction side velocity profile. This meant that this area of the wake did not contribute to the value of θ_{TE} , resulting in an underestimation of the profile drag.

The final approach which was used in this analysis was to describe the variation in external velocity as a step function, with the step occurring at the y co-ordinate of the minimum flow velocity. This corresponds to the usual assumption in boundary layer theory that the static pressure does not vary through the boundary layer, and effectively treats the pressure and suction surface profiles as separate boundary layers. This assumption is less than ideal, but was the best solution in the time available for this project.
The momentum thickness θ_{TE} was then calculated with the two values of U_{TE}, using the usual relationship:

$$\theta_{TE} = \int(1 - \tfrac{u}{U})d\eta$$

C_{dv} was then calculated using equation 2, employing the relationship between U_{TE}, and U_{∞} given by Bernoulli's equation.

References

1. Mueller, T.J. et al., 'Low Reynolds Number Wind Tunnel Measurements: The Importance of Being Earnest'. Paper 14, Aerodynamics at Low Reynolds Numbers conference, Royal Aeronautical Society, 1986.

2. Simons, M., 'The Use of Wind Tunnel Data in the Design of Radio Controlled Contest Sailplanes'. Paper 20. Aerodynamics at Low Reynolds Numbers conference, Royal Aeronautical Society, 1986.

3. Drela, M., 'Aerodynamics of Human-Powered Flight'. Annual Review of Fluid Mechanics 22: 93-110, 1990.

4. Drela, M.; 'Low-Reynolds-Number Airfoil Design for the M.I.T: Daedalus Prototype: A Case Study'. Journal of Aircraft volume 25, number 8, pages 724-732: American Institute of Aeronautics and Astronautics, Inc. Washington DC, 1988.

5. Cornish, J.J., 'Airfoil Analysis and Synthesis Utilizing Computer Graphics', SAE Paper 670845,1967

6. Liebeck, R.H., 'Low Reynolds Number Airfoil Design at the Douglas Aircraft Company'. Paper 7, Aerodynamics at Low Reynolds Numbers conference, Royal Aeronautical Society, 1986

7. Eppler. R. and D.M. Somers, 'A Computer Program for the Design and Analysis of Low-Speed Airfoils'. NASA TM-80210, 1980.

8. Liebeck, R.H., 'Low Reynolds Number Airfoil Design for Subsonic Compressible Flow'. Low Reynolds Number Aerodynamics - proceedings of the conference Notre Dame, Indiana, June 1989: Springer Verlag, 1989.

9. Drela,M. and M.B. Giles, 'ISES: a Two-Dimensional Viscous Design and Analysis Code'. AIAA Paper 87-0424, Jan. 1987.

10. Drela, M., ' XFOIL: An Analysis and Design System for Low Reynolds Number Airfoils'. Low Reynolds Number Aerodynamics - proceedings of the conference Notre Dame, Indiana, June 1989: Springer Verlag, 1989.

11. Evangelista, R., R.J. McGhee and B.S. Walker, ‘Correlation of Theory to WindTunnel Data at Reynolds Numbers Below 500,000’. Low Reynolds Number Aerodynamics - proceedings of the conference Notre Dame, Indiana, June 1989: Springer Verlag, 1989.

12. Donovan, J.F. and M.S. Selig, ‘Low Reynolds Number Airfoil Design and Wind Tunnel Testing at Princeton University’. Low Reynolds Number Aerodynamics - proceedings of the conference Notre Dame, Indiana, June 1989: Springer Verlag, 1989.

13. Weston, N.. ‘Some Preliminary Results from a Programme of Flight Research with a Low Reynolds Number Aircraft. Royal Aeronatical Society Symposium on Human Powered Flight, January 1996.

14. Wortmann, F.X., ‘Airfoil Design for Man Powered Aircraft’. Massachusetts Inst. of Technology, Low Speed Symposium, 1974.

15. Mueller, T.J., ‘Low Reynolds Number Vehicles’. AGARDograph No. 288. NATO, February 1985.

16. Liu, H.T.,’Atmospheric Turbulence and Gust on the Performance of a Wortmann FX 63-137 Wing’. Paper 9, Aerodynamics at Low Reynolds Numbers Conference, Royal Aeronautical Society, 1986.

17. Liu, H.T.,’Atmospheric Turbulence and Gust on the Performance of a Wortmann FX 63-137 Wing’. Paper 9, Aerodynamics at Low Reynolds Numbers Conference, Royal Aeronautical Society, 1986.

18. Mueller, T.J. et al., ‘Low Reynolds Number Wind Tunnel Measurements: The Importance of Being Earnest’. Paper 14, Aerodynamics at Low Reynolds Numbers conference, Royal Aeronautical Society, 1986.

19. Lewis, R.I., ‘Vortex Element Methods for Fluid Dynamic Analysis of Engineering Systems’ Cambridge Engine Technology Series. First Edition. Cambridge: Cambridge University Press, 1991.

20. Fletcher, C.A.J. ,’Computational Techniques for Fluid Dynamics’. Second Edition, Vol.2, Berlin: Springer-Verlag, 1992.

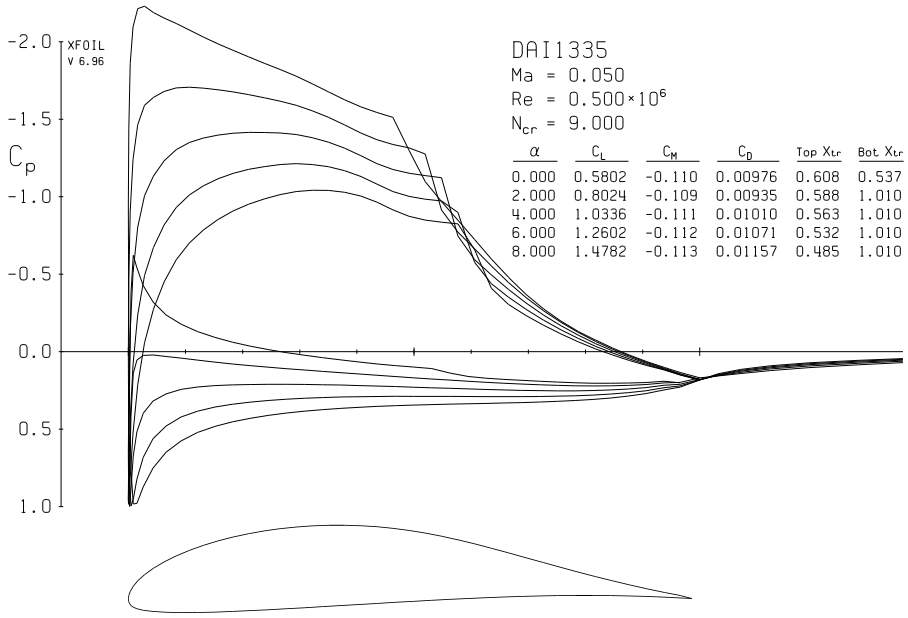

Fig 1.1 DAI 1335 Aerofoil

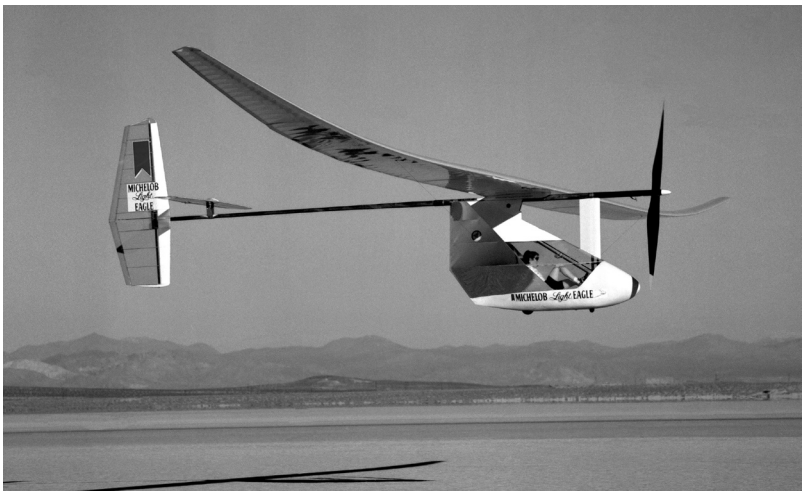

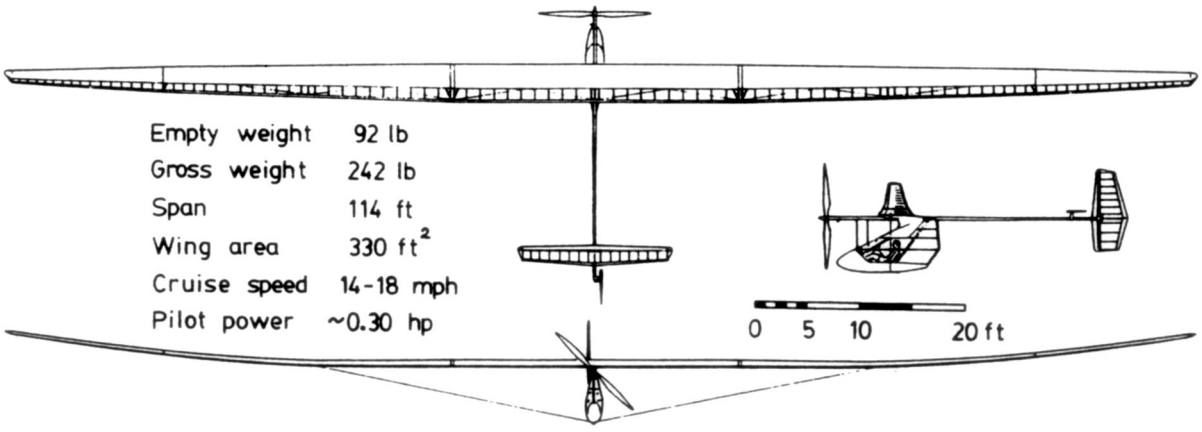

Fig 1.2 MIT Light Eagle HPA

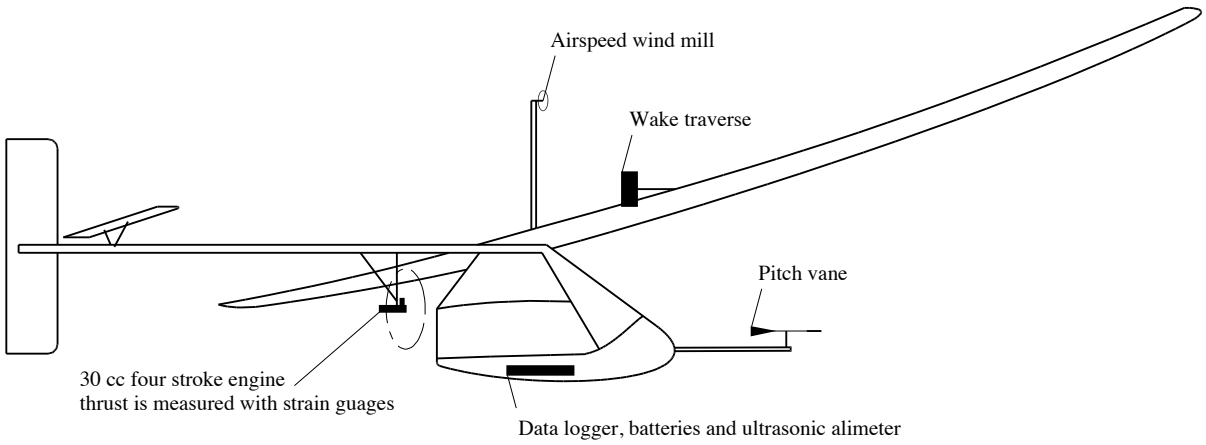

Fig 1.3 Airglow HPA with instrumentation

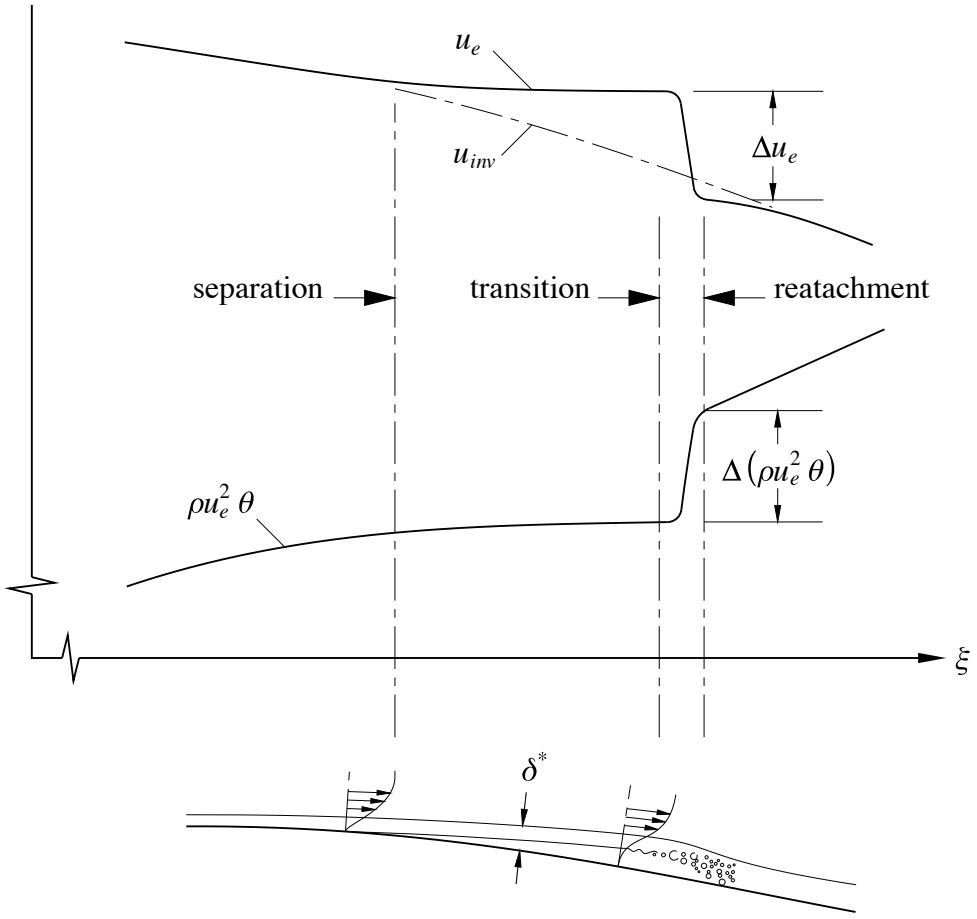

Fig 2.1 Edge velocity and momentum deficit jumps due to separation bubbles

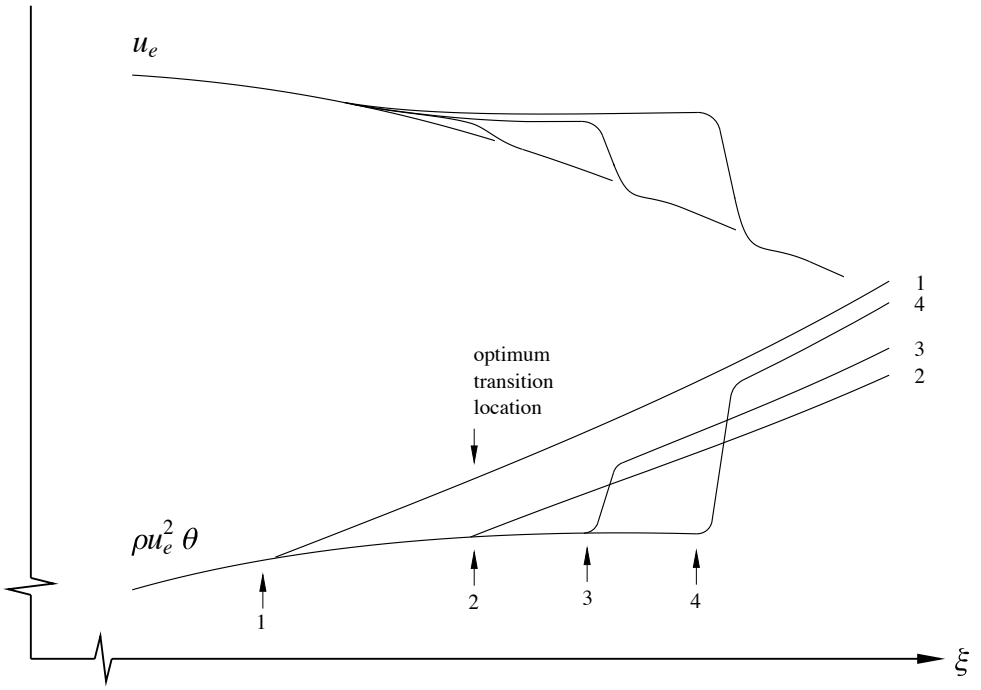

Fig 2.2 Effect of transition location on bubble size and loss.

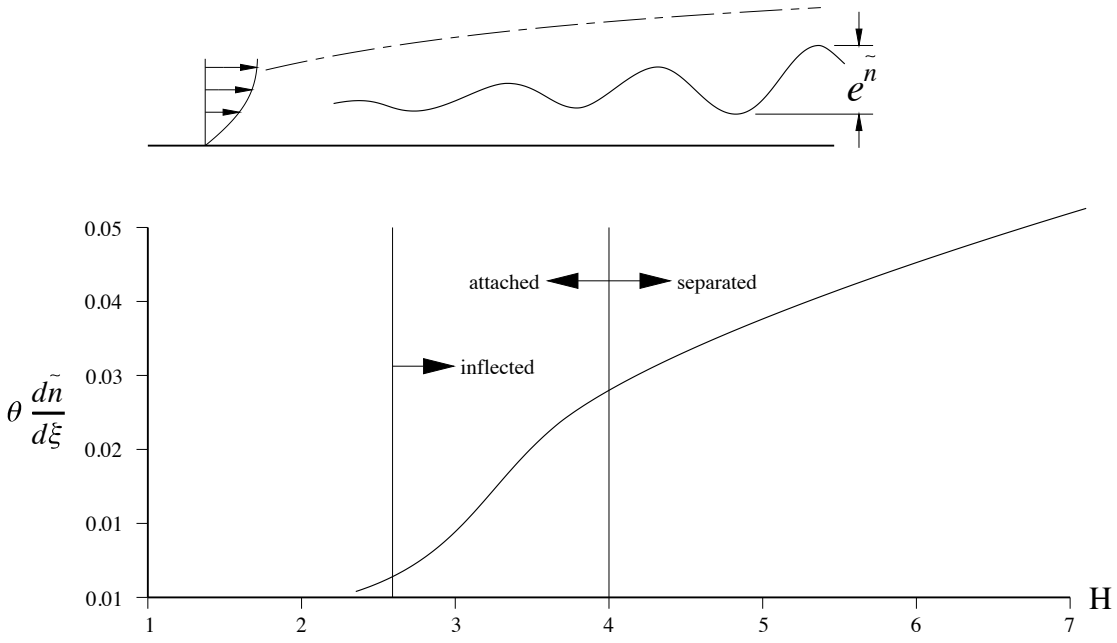

Fig 2.3 Growth rate of most amplified Tollmien-Schlichting disturbance.

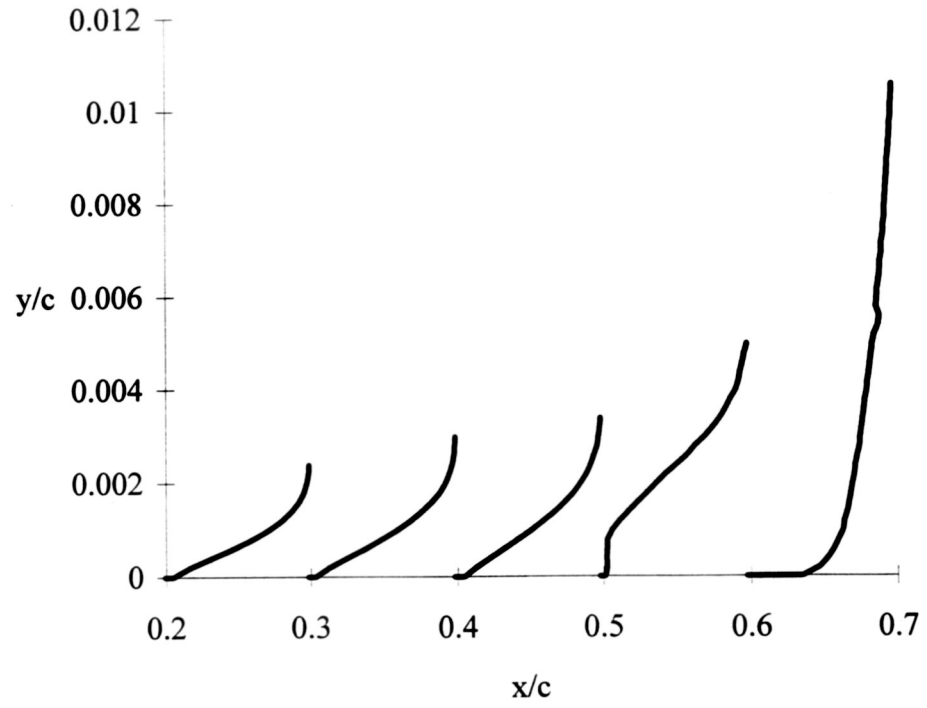

Fig. 5.1.1 Mean velocity profiles on suction surface at alpha = 4.

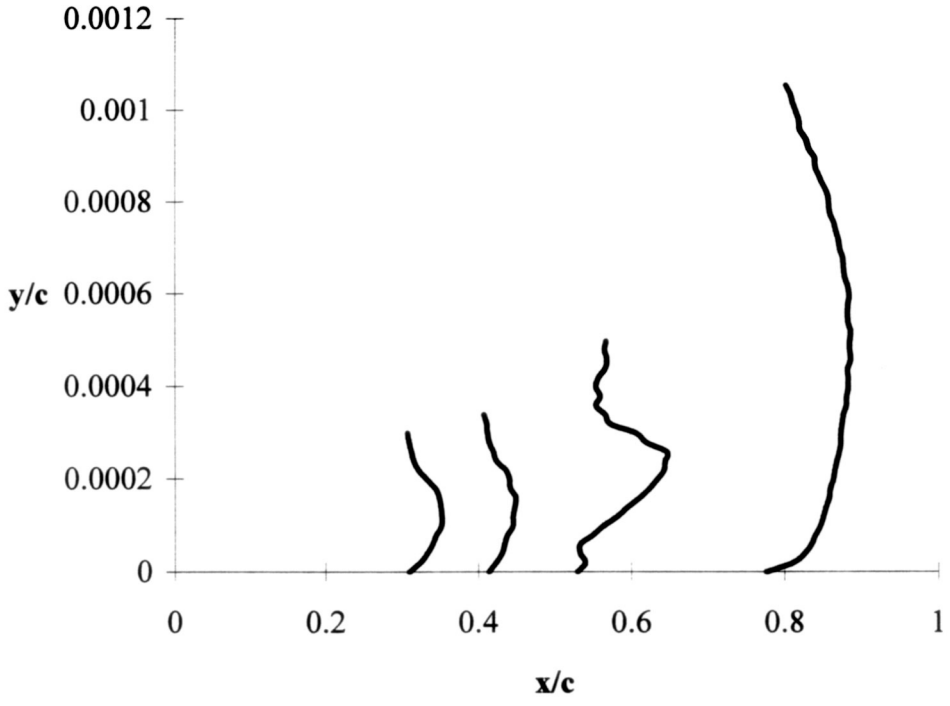

Fig. 5.1.2 Turbulence intensity profiles on suction surface at alpha = 4

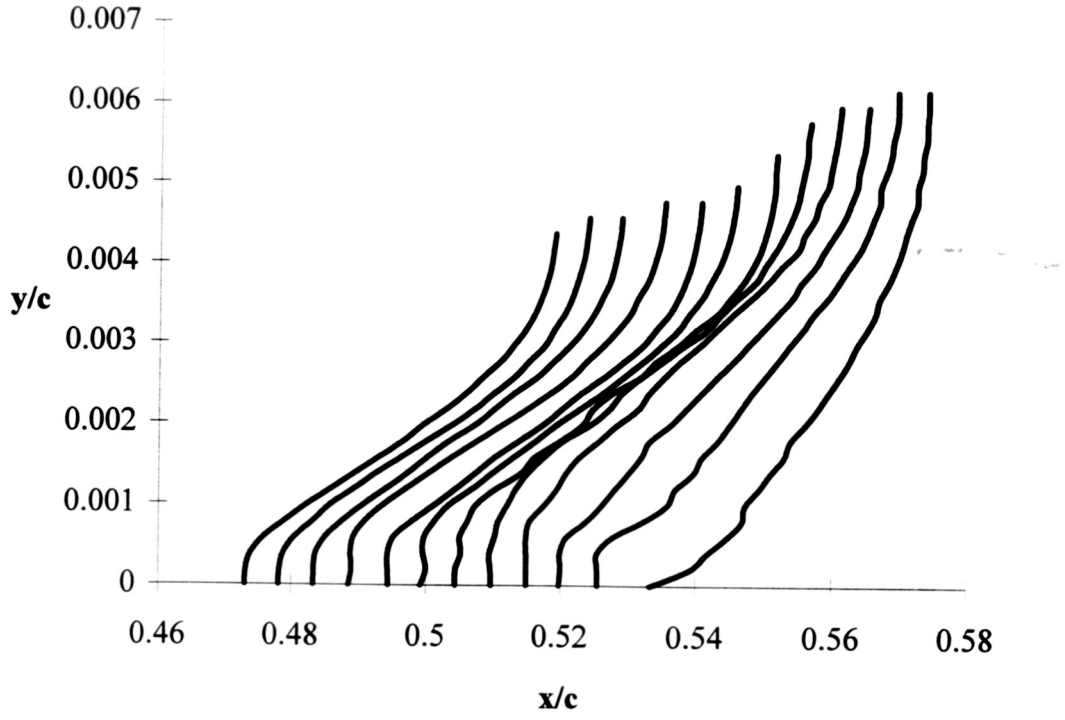

Fig. 5.1.3 Mean velocity profiles through separation bubble at alpha = 4

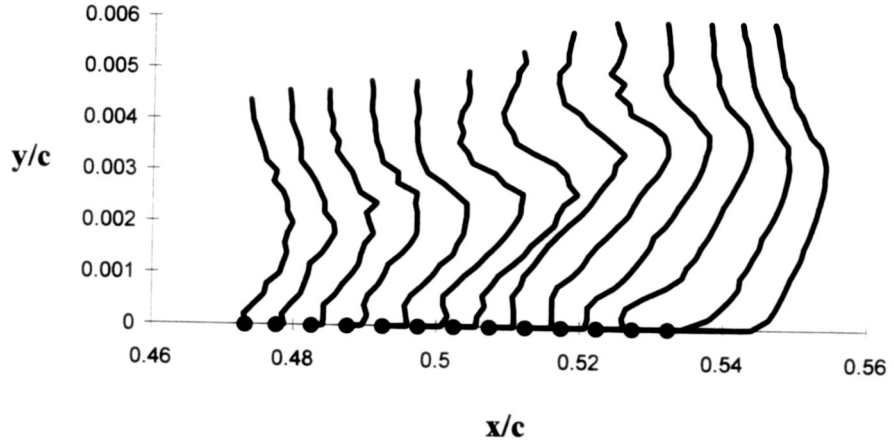

Fig. 5.1.4 Turbulence intensity profiles through separation bubble at alpha = 4

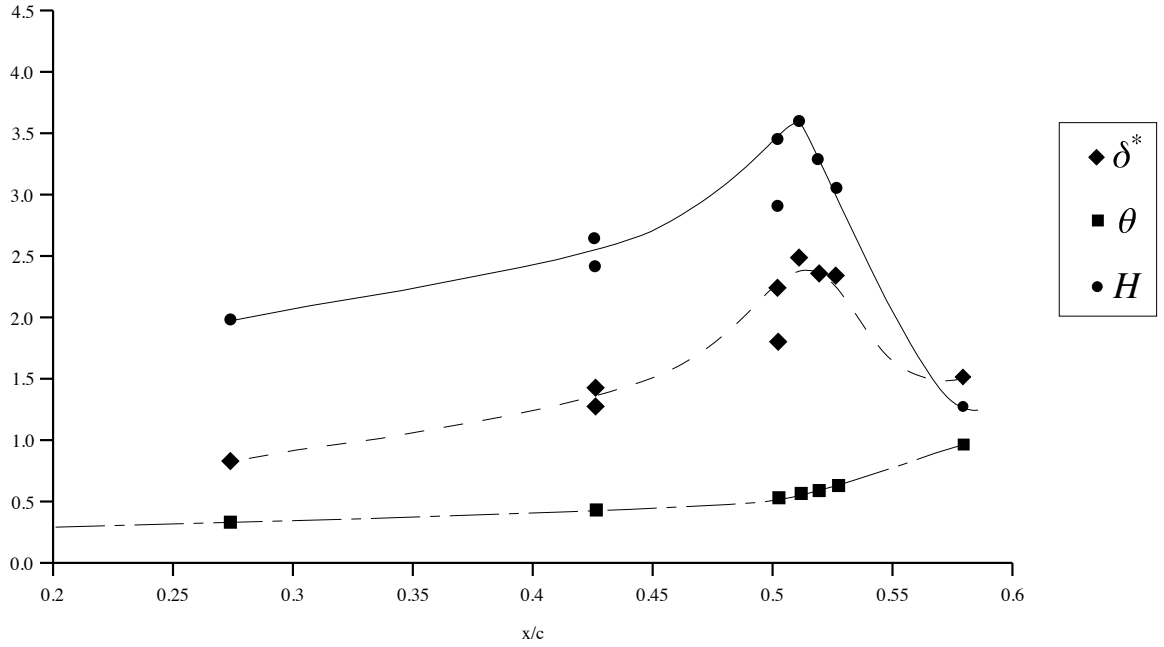

Fig. 5.1.5 Boundary layer parameters on suction surface at alpha = 0 degrees

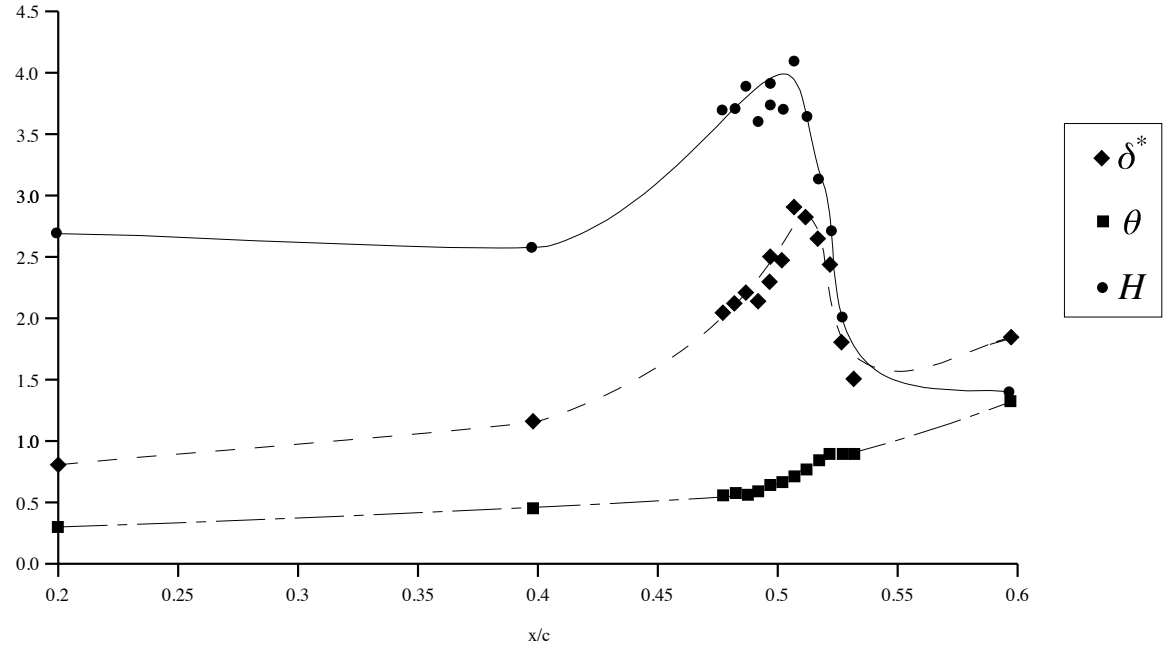

Fig. 5.1.6 Boundary layer parameters on suction surface at alpha = 4 degrees

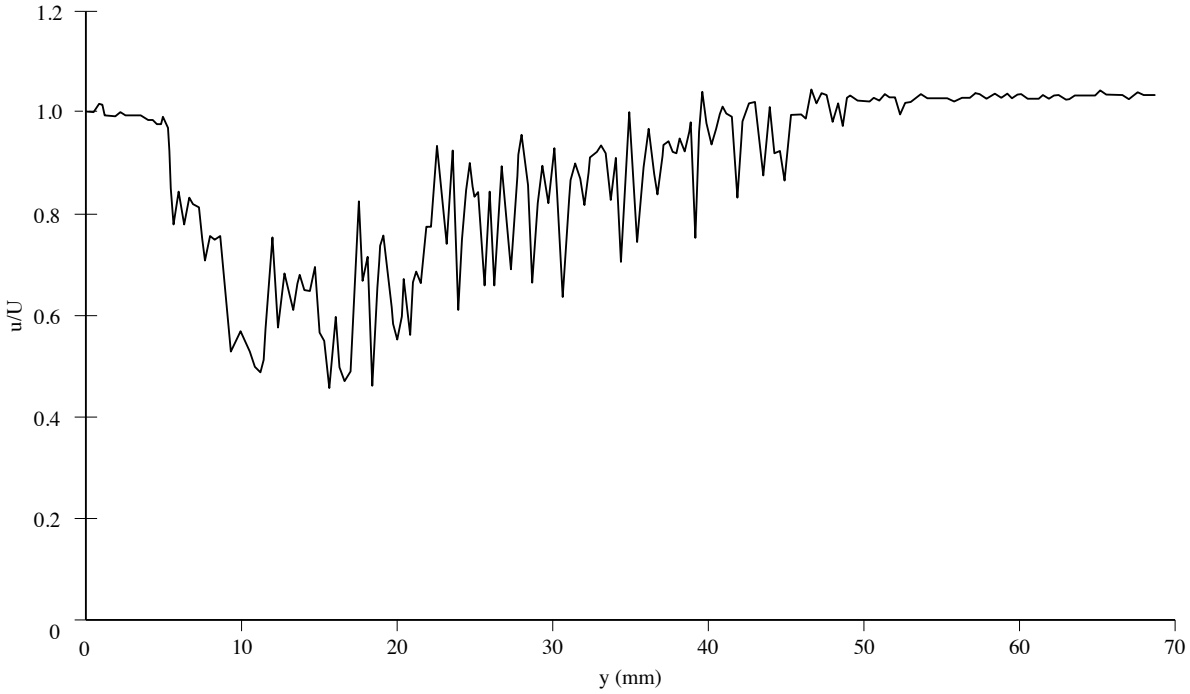

Fig 5.2.1 Wake profile for alpha = 4, rms free stream turb. Intensity = 0.26%, clean wing

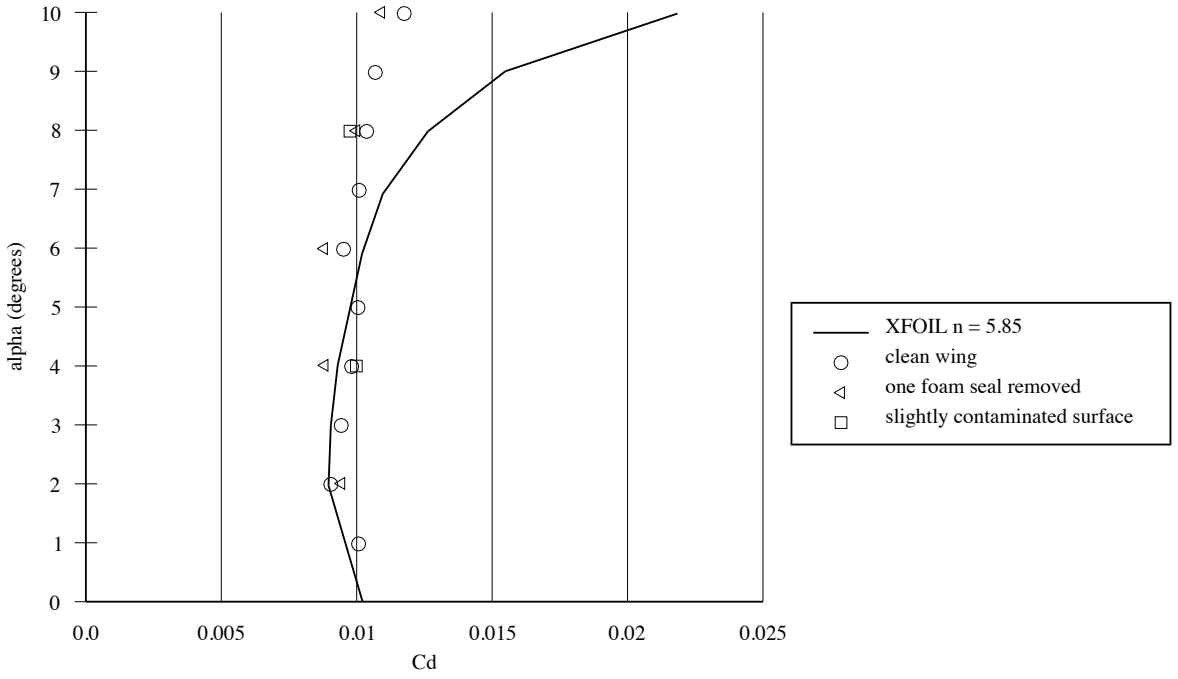

Fig 5.2.2 Theoretical and experimental drag values for rms free stream turb. Intensity = 0.26%

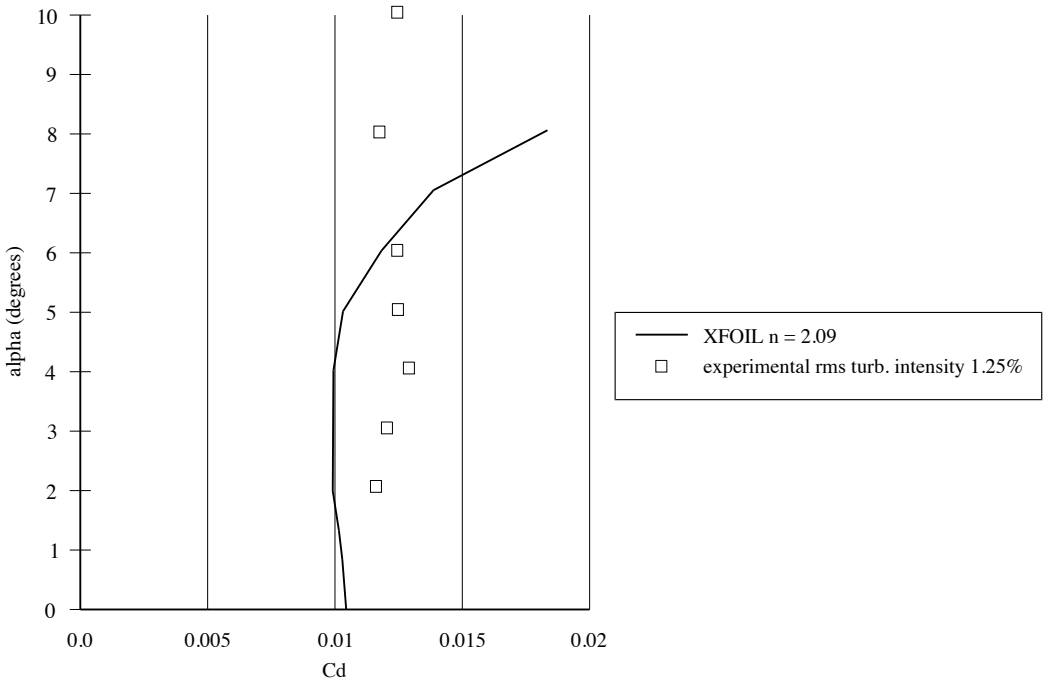

Fig 5.2.3 Theoretical and experimental drag values for rms free stream turb. Intensity = 1.25%

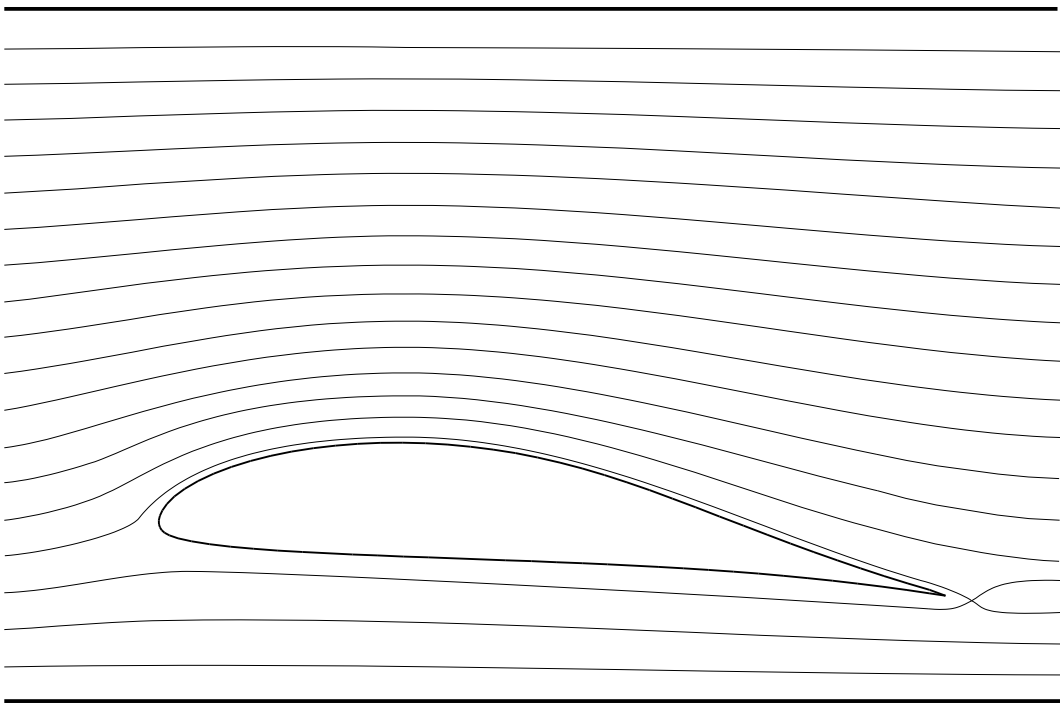

Fig. A.1 Inviscid flow prediction of wing in Low Turbulence wind tunnel, offset from centreline. Note streamlines at trailing edge.

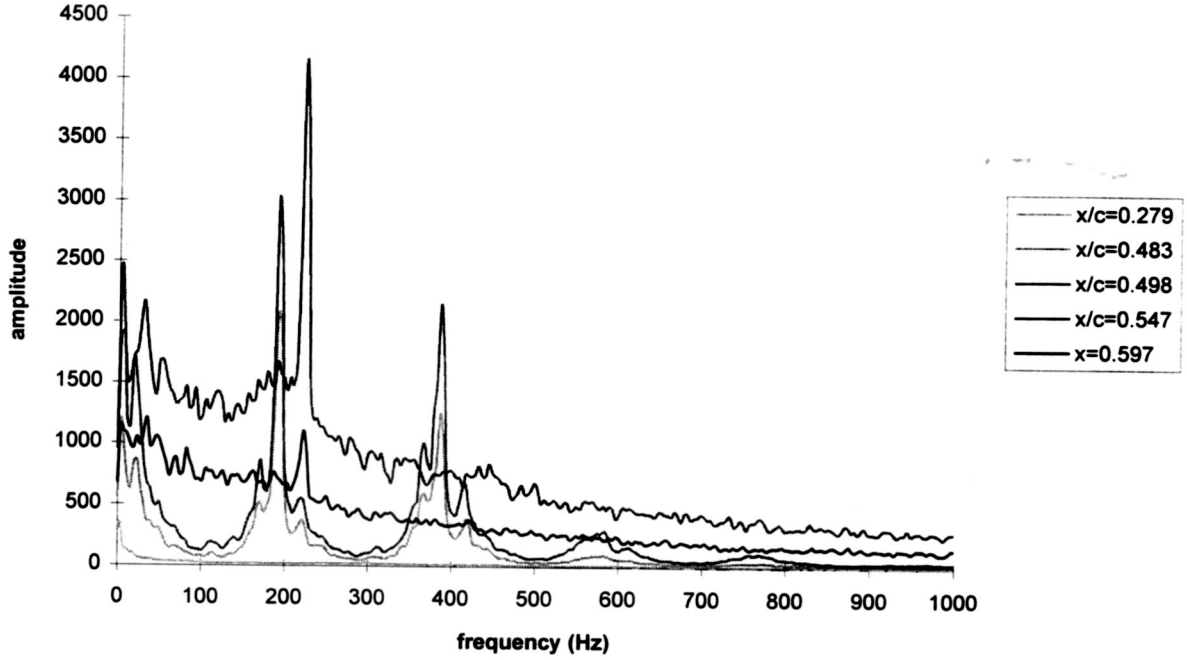

Fig. 5.1.7 Turbulence spectra through transition region at alpha = 4

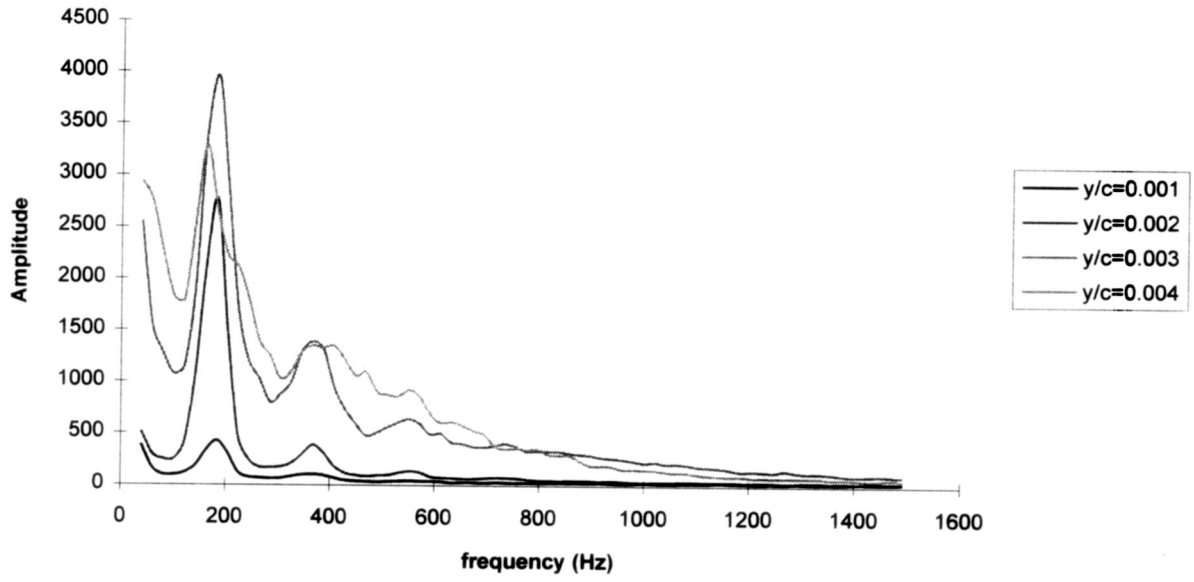

Fig. 5.1.8 Turbulence spectra through cross-section of boundary layer at alpha = 4

Note. This project won the RAeS HPAG Robert Graham prize in 1996

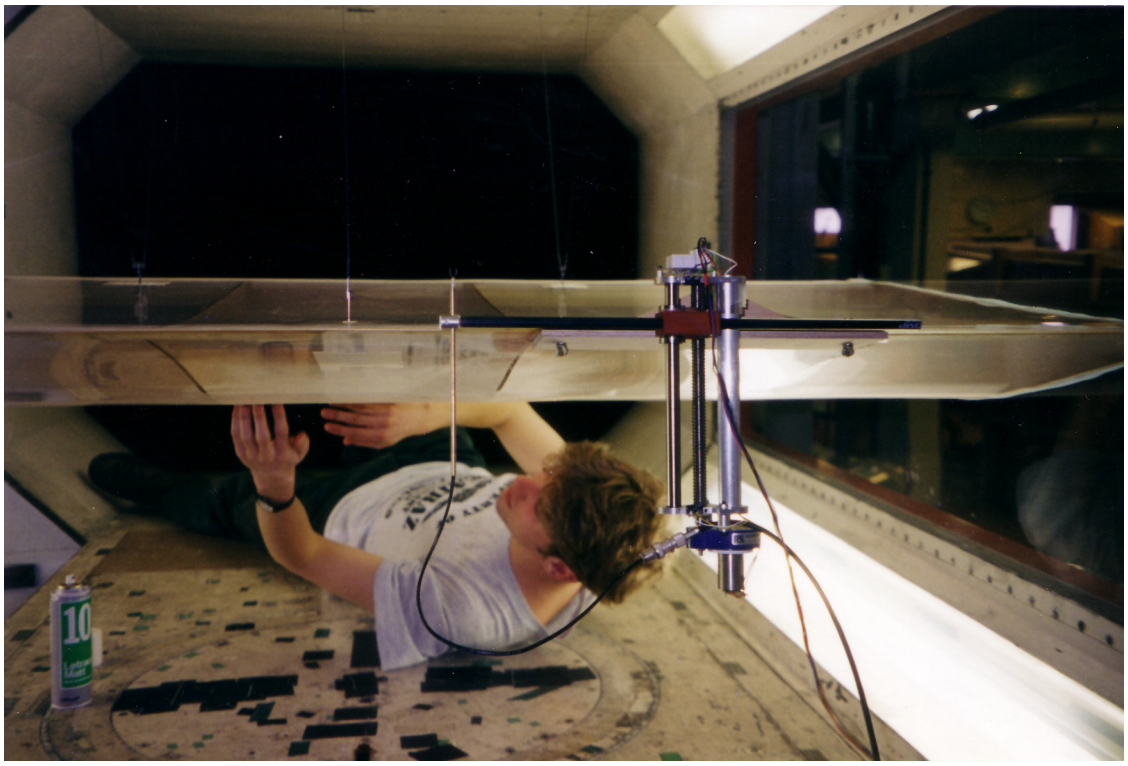

Top: Richard in the Markham wind tunnel. The wake traverse can be seen attached to the trailing edge of the wing section. Bottom: Richard in the low turbulence wind tunnel checking the position of the hot wire anemometer probe.